N86-28287

The New 34-Meter Antenna

M. F. Pompa
TDA Engineering

This article describes the new 34-m high efficiency Azimuth – Elevation antenna configuration, including its features, dynamic characteristics and performance at 8.4-GHz frequencies. The current-technology features of this antenna produce a highly reliable configuration by incorporation of a main wheel and track azimuth support, central pintle pivot bearing, close tolerance surface panels and all-welded construction. Also described are basic drive controls that, as slaved to three automatic microprocessors, provide accurate and safe control of the antenna's steering tasks.

At this time antenna installations have been completed at Goldstone and Canberra and have operationally supported the Voyager – Uranus encounter. A third installation is being constructed currently in Madrid and is scheduled for completion in late 1986.

I. Introduction

The addition of the 34-m Azimuth – Elevation high efficiency antennas was undertaken as a result of early Mark IVA Project studies directed at providing increased DSN aperture capacity to support the Voyager – Uranus encounter. Furthermore, the presence of these antennas – one each at the Deep Space Communications Complexes (DSCCs) located at Goldstone, Canberra and Madrid – would provide support for the increased quantity of high priority missions in the late 1980's to early 1990's period. Imaging data, 8.4-GHz telemetry and science data are the primary data yields sought at the Voyager – Uranus encounter and beyond, and can be expected only with the 34-m Az – El antennas addition, when arrayed with the existing 64-m antenna.

A principal contending option for providing the netwide added aperture was the collocation of existing 26-m STDN antennas, including their enlargement to 34 m, a project similar to the earlier S – X (26-m to 34-m) upgrade project. Final cost and performance comparisons favored the new 34-m Az – El antenna, and implementation of this configuration was initiated in April 1982.

II. General Features and Performance Capacities

The 34-m diameter, Az – El configuration is a quasiparaboloid surface of revolution whose RF reflective surface has a focal length-to-diameter ratio of approximately 0.325, and a cassegrain RF optics path consisting of a quadripod structure, adjustable subreflector, and an interchangeable feedcone similar to those used on other DSN antennas. The antenna is steerable in azimuth and elevation with intersecting axes. These highly recognizable features are shown in Fig. 1.

The antenna structure is designed to maximize stiffness, minimize surface distortions and provide accessibility for maintenance. In order to maximize traction and to minimize wheel loadings, a four wheel azimuth turntable with a square platform is used. This azimuth turntable has self-aligning wheels and a machined track to minimize stress concentrations.

The reflector structure is a triangulated truss system constructed of standard angles and tubes. In order to minimize load induced surface distortions, the reflector is attached to the pedestal via a trussed elevation wheel structure which provides eight equally still mounting points to the reflector and isolates the counterweight loads from the reflector.

Table 1 is a summary of the antenna specifications and characteristics of the 34-m AZ – El configuration.

III. Physical Description

A. Azimuth—Elevation Structure and Drive Equipment

1. Foundation and alidade structure.

a. Basic Support. The fundamental support for the entire antenna is the azimuth rail and ring resting on an earth and concrete foundation with spread footings. (See Figs. 2 and 3.) Radial rigidity for the ring structure is provided by four (4) radial beams tied in at the center pintle bearing support. Minimum compressive strength of the concrete in the ring beam is 34,475 kPa (5000 psi).

b. Alidade structure. The alidade structure illustrated in Fig. 4 supports all components above the four (4) azimuth wheels. It is a triangulated structure with a square base interfacing with the azimuth wheels over the track and the center pintle bearing. The square base and lateral plane of the alidade are braced for structural stabilization.

The bracing in the base frame includes radial members framed into the center pintle bearing so that the alidade transfers all loads to the four azimuth wheels and pintle bearing. A plane of bracing is also included near the elevation drives (top plane) to stabilize the working points of the alidade side frames.

The alidade is constructed of standard wide flange structural beams. Standard bolted field flange splices are used at installation, after which the field joints are welded to prevent any joint slippage. Wide flange sections are used to provide a good stiffness to weight ratio for bending loads, which is extremely important in the base frame that interfaces with the four azimuth wheels and pintle bearing. Wide flange sections also are not susceptible to the internal corrosion problem encountered in the tubular sections.

The top plane of the alidade structure serves to mount the two elevation bearings, elevation wheel and drive motors. These bearings support and actuate the entire tipping structure, i.e., main reflector, quadripod, subreflector, counter weights, etc. These are discussed further in Section III.A.2.

c. Azimuth radial bearing. The azimuth radial pintle bearing, illustrated in Fig. 5, is a single-row ball, four point contact bearing equipped with replaceable split grease seals and lubrication ports for greasing the rolling elements. It is the main stabilizing point of the antenna's rotational motion.

The inner ring of the radial pintle bearing is bolted to an adapter ring plate which is securely fastened to the concrete center pedestal. The outer ring of the pintle bearing has six flexure plate assemblies bolted to it which are also bolted to the diagonal members of the alidade base frame. The flexure plate assemblies transmit lateral forces from the alidade base frame to the radial bearing, since the flexure plates are relatively stiff when loaded radially. Small vertical thrust loads are transmitted to the radial bearing by virtue of the flexibility of the flexure plate assemblies. The azimuth radial bearing has sufficient capacity to carry radial loads induced by misaligned azimuth wheels in addition to radial loads induced by winds.

The azimuth radial bearing has an outside diameter of 240 cm (94.50 in.) and an inside diameter of 200 cm (78.88 in.).

d. Azimuth bearing track. Vertical or thrust loading is carried by the azimuth bearing which consists of a self aligning wheel and track configuration.

The mean radius of the azimuth bearing track is 982 ± 0.635 cm (386.7 ± 0.25 in.). The annular ring segments are 12.2 cm (4.80 in.) thick and 36.6 cm (14.40 in.) wide.

The azimuth bearing track shown in Fig. 6 consists of an annular ring made of low carbon steel and formed by 16 segments leveled, grouted into place, and capped with hardened wear strips with mitered ends.

After the ring segments are aligned and held in position, drypack grout is placed between the ring elements and foundation. The wear strips are 3.05 cm (1.20 in.) thick and 27.94 cm

(11.0 in.) wide, and the edges and ends of the wear strips and ring segments are sealed with RTV silicone for corrosion protection.

e. Azimuth bearing wheel assembly. Each of the four corners of the alidade base structure is supported by a wheel assembly. The two wheel assemblies nearest the reflector (when the reflector is in its near-horizon position) are the powered (driving) assemblies, as shown in Fig. 7. Each wheel assembly consists of a wheel and shaft supported by two spherical roller bearings contained within a wheel housing.

The wheels are 60 cm (23.62 in.) in diameter and 14.4 cm (5.67 in.) wide with a tapered wheel rim in order to roll true on the circular track. The wheel is shrunk fit on a wheel axle and mounted in a housing which is supported by two pairs of flexure links, thus allowing full width alignment of the wheel on the track.

Provision is made for jacking each corner of the alidade base frame for relieving the loads on the wheel assembly attachment bolts for wheel alignment.

f. Azimuth drive assemblies. Each of the two powered wheel assemblies is driven by two 3.2 kW (5 hp) direct current (DC) drive motors, also shown in Fig. 7. The drive axle ends are mounted to the output shaft of a 649:1 ratio speed reducer which is flange mounted to the wheel assembly housing.

A double C-face disc brake coupler is mounted to each DC drive motor and to the input shaft of each speed reducer. Each DC drive motor is equipped with a tachometer.

The total ratio from the DC drive motor output shaft to the antenna axis is 21,250:1, resulting in an antenna azimuth speed of 0.49 deg/s when the DC drive motor is operating at 1750 rpm.

2. Elevated and tipping structure assemblies.

a. Elevation bearing assembly. The elevation axis bearings consist of two spherical roller bearings which are mounted in housings bolted to the top of the alidade structure. The elevation shafts are fixed to the reflector back-up structure and the bearings are mounted on the shafts as shown in Fig. 8.

Split grease seals with seal retainers are mounted in the bearing housing on each side of the bearing. The seals can be removed and replaced while the bearing and housing are in place by using standard hydraulic pumps and gear pullers. At the outer end of each elevation shaft, flexible coupling connects the angle encoders in such a way that the encoder mount stiffness is consistent with the encoder accuracy requirements.

b. Elevation wheel and counterweights. The elevation wheel structure is a welded plate girder braced by a trussed framework as shown in Fig. 8. It is especially configured to provide uniform support for the reflector at all orientations. The elevation wheel structure is a steel space frame that supports the primary reflector structure, the elevation counterweights, the drive bullgear, and the elevation drive. It is supported by the elevation bearing assembly. The back rim of the elevation wheel consists of a steel flange for supporting the elevation bull gear. This gear is shimmed against the wheel to adjust for radial run-out and for lateral position. The bull gear is bolted to the wheel to prevent tangential slippage during operation.

c. Elevation drive carriage. The elevation drive carriage consists of a housing which supports two drive pinions arranged with their axes parallel and spaced circumferentially apart, meshing with the elevation bullgear. The drive carriage is supported by two tangent links connected to alidade joints. Each pinion is driven by a Sumitomo Cyclo Drive Model 19045, whose speed reducer ratio is 385:1 and whose output shaft is keyed to the pinion. The two reducers are mounted on opposite sides of the bullgear to provide a balanced elevation drive carriage. A fail-safe brake is mounted on the input side of each reducer and two 6.4-kW (10-hp) DC drive motors with tachometers are mounted to each brake. Air blowers are provided so that cooling air is ducted over each drive motor. The total ratio of the elevation drives is 21,988:1, which corresponds to a slewing speed of 0.48 deg/s.

d. Elevation gear. The elevation bullgear is composed of gear segments which are mounted on the elevation wheel structure. The elevation gear is formed to provide a surface for back-up rollers which is concentric to the pitch diameter of the gear teeth, insuring proper mesh of the gear and pinions. The elevation gear has a pitch radius of 653 cm (257 in.) and a diametral pitch of 2.

e. Primary reflector structure. The reflector structure supports the aluminum reflector panels' quadripod and subreflector. The reflector is supported from the elevation axis by the elevation wheel structure. This structure consists of twenty-four radial trusses extending out from a welded center hub. The reflector trusses and interconnecting chords are fabricated of welded square steel tube sections. The resulting space frame acts to distribute asymmetric wind pressure loads and provide torsional resistance; it is illustrated atop the alidade structure in Figs. 9 and 10.

The primary reflector with its total support structure and mechanical systems has a natural frequency of 1.5 Hz (locked rotor system), while the quadripod subreflector subset has a natural frequency of 1.0 Hz.

f. Reflector panels and assembly. The main reflector, as configured by the contiguous positioning of individual panels, presents a homologous paraboloid for improved microwave efficiency. The individual panels are manufactured from 6061-T6 aluminum and have a skin thickness of 1.78 mm (0.070 in.). All surface panels inside the 26-m (85-ft) diameter are solid surfaces; the panels outside this diameter have a perforated surface with a porosity of 40% provided by 3.175-mm (0.125-in.) holes in a diamond pattern. The solid surface panels can support a 137-kg (300-lb) shoe load with no permanent deformation; similarly, the perforated panels can support a 91-kg (200-lb) shoe load on any point of the surface. The panels are manufactured with a ±0.305 mm (±0.012 in.) surface tolerance. Details of the assembled panel array are shown in Fig. 11, and a typical panel sector is shown in Fig. 12.

g. Quadripod – apex structure. The quadripod – apex structure serves to support the 381 cm (150 in.) diameter subreflector, and its 3-axis drive system with its associated support structure. Aperture blockage is 5%. The quadripod legs have a trapezoidal cross-section, consisting of square tubing in the corners with square tubing or plate webbing as shown in Fig. 13. Two legs enclose a 12.7-cm (5-in.) diameter conduit pipe that houses the control cables to the subreflector drive system at the apex.

h. Subreflector. The aluminum subreflector is fabricated out of six individual panels, each being supported from a trussed backup structure in the assembled configuration. All surface gaps between individual panels and between the panels and the center tooling plug are covered with one layer of Kapton adhesive tape, overlaid by one layer of aluminum adhesive tape to form a continuous conducting surface. A center hub is provided for mounting a rotating sweep template to verify the surface accuracy of 0.305 mm (0.012 in.) RMS.

The assembled and mounted subreflector assembly is shown in Fig. 1, atop the quadripod structure.

i. Subreflection positioning mechanism. The subreflector position mechanism serves to compensate and minimize systematic loss of gain due to gravity deformation of the antenna primary structure, quadripod structure and primary reflector surface when operating at the various elevation positions. The subreflector positioner coordinate system is as shown below:

+Z axis, away from primary reflector

+X axis, to right (when looking in +Z axis direction)

+Y axis, up (when looking in +Z axis direction and primary reflector is at zenith)

The positioner can adjust the central coordinator points of the subreflector from 0 to ±7.1 cm (±2.8 in.) along each of the 3 orthogonal axes mentioned above.

IV. Antenna Drive Control Command and Monitoring

The antenna control as required to meet the Mark IVA reconfiguration is accomplished through the use of a system of interconnecting microprocessor computers. At one end of the controls network are the Antenna Drive Assembly (ADA) microprocessors located on the antenna to provide antenna drive actuator signals (through servo control loops), monitor equipment status, and provide limit and fault energization. At the other end are two Modcomp computers comprising prime and backup Antenna Pointing Assembly (APA) processors located in the Signal Processing Center (SPC). The APA stores data for the pointing process, e.g., it stores trajectory prediction points profiles, systematic error correction tables, transformation of coordinates, and monitor data back to the Area Routing Assembly (ARA), MDA, and NTK. One primary computer connection exists between the APA and ADA which is embodied in the Antenna Control Subassembly (ACS). In effect the ACS, located on the antenna, is an extension of the APA, and operates to store predict tables, perform interpolation between predict points, combine position commands to obtain a final pointing position, and provide antenna and subreflector positions feedback.

A detailed treatment of the APA and ACS will be covered in a future paper. In this current article the discussion will be on the drive and control assemblies and microprocessors. Figure 14 shows a block diagram of the major control assemblies' microprocessors, including simplified interconnecting routes and locations. These assemblies are required for complete antenna control and pointing. To the left are the pointing process computers and to the right are the front end area (FEA-Antenna) microprocessors and drive controls. The FEA mounted assemblies, incorporating the Antenna Servo Controller (ASC), the Antenna Control and Monitor (ACM), Subreflector Controller (SRC) and servo control chassis, will be discussed further as to purpose, function and performance.

A. Basic Drive Controls and Chassis

As previously described, electric motors and actuators, acting through appropriate gearing, provide the basic motion to the antenna about the azimuth and elevation axis and to the subreflector. These prime movers are augmented and modulated by the use of limit switches, relays, brakes, field modulators, wave shapers, sensors, etc. which may be manually energized to provide the desired torque and counter torque. The switching and interfacing for all these devices takes place at the Drive Control Cabinet, Subreflector Drive Cabinet and Field Interface Module (FIM). From these modules commands and status are intercommunicated with the ASC, ACM and SRC microprocessors which provide the signal processing for automated servo control of the antenna. Therefore signal voltages are generated from the various input error signals, or manual slew commands, which flow to the ASC and return to the Drive Cabinet for amplification and gain processing and thence to the drive motors.

The current (drive motor armature) and velocity servo loops are closed in the Drive Control Cabinet.

B. ASC

The ASC accepts position commands from the ACS and closes the position servo loop for the main driving assemblies. It also issues rate and limit commands, and provides antenna monitoring functions for status determination as required for appropriate operation and personnel safety.

The ASC chassis contains an Intel MULTIBUS based microprocessor and the custom interface electronics required to interface the chassis to the antenna mounted devices. The microprocessor consists of four standard MULTIBUS compatible microprocessor boards together with the card cage and the motherboard.

A large-error algorithm and a small-error one are used for rate command calculation. The large-error algorithm is utilized when the calculated rate command error is greater than 0.05 deg/s and the position error is greater than 0.03 deg (nominal values); the small-error algorithm is used at values less than those given for the large-error one. After the rate command is calculated by one of these algorithms, it is then processed by the rate and acceleration limiter section.

Whichever algorithm is currently being used, the current antenna position is always monitored by strobing the encoder of an axis every 50 ms. Validity of the data is verified by the status provided by the encoder board itself. Under normal circumstances, the converted encoder position is reported to the ACS controller and used as input to the position loop.

Commanded positions are received by the ASC controller in one of the following forms: MOVE commands from the ACS assembly, STOW, or STOP. The primary purpose of the commands is to generate a new commanded position. In the case of the MOVE commands from the ACS assembly which are used only during tracking conditions, the commanded position dictated by the ACS is interpolated over twenty 50-ms periods.

C. Antenna Subreflector Controller (SRC)

The subreflector is positioned in its three orthogonal axes by a system of motor driven ballscrew jacks and linkages. In normal operation the motors are energized to correct the subreflector position or magnetically detented to hold the subreflector against gravity or wind loads. The SRC operates to achieve the necessary motion and position control of the subreflector.

The SRC accepts position commands from the ASC and closes the position loop for the drive assembly. The ASC also provides antenna position data to the SRC. Limit switches, brakes and a self-diagnostic function are also monitored in the SRC.

The SRC controller is located in a single chassis assembly designated 3763/ANT-310 and containing the following four circuit boards:

(1) 16-bit CPU board (A1A1)

(2) 4-channel intelligent communication board (A1A3)

(3) PROM board (A1A4)

(4) Digital input/output board (A2A1)

Each of these circuit boards communicates with the others through the Intel Multibus.

D. Antenna Control and Monitoring (ACM)

The ACM program has three major functions:

(1) Configuration and Control

(2) Monitoring and Alarm Reporting

(3) Data Collection

On the 34-m Az – El antennas, there are no operator-selectable configuration parameters except enabling/disabling of alarm condition reporting and entering the criticality of a track. The ACM starts up or shuts down the drive cabinet electronics, motor controllers, and power supplies on command. Such startup and shutdown commands can be entered from the local terminal, or from a terminal connected to any upstream computer. They are also generated automatically by the APA.

Whenever the antenna is up and running, the ACM monitors various sensors to determine whether the antenna is operating properly. If any discrepancies are detected, the ACM will generate appropriate event messages designed to ensure the safety and integrity of the antenna and personnel.

The ACM constantly collects analog and digital data from the Field Interface Module (FIM) and periodically sends this information upstream for analysis or logging. In addition, monitor point values may be requested by name.

The ACM physical makeup consists of the following equipment:

(1) A standard chassis with cardcage and power supply

(2) iSBC-86/14 master CPU card

(3) iSBC-337 Floating Point Arithmetic piggyback module

(4) Two (2) iSBC-464 PROM expansion cards

(5) MCM-8086 core card

V. Microwave Testing and Performance

Gain values were measured during dedicated engineering tests by scanning of various radio sources. Antenna focusing was also determined while stepping the subreflector through the range of its excursions. Operating temperatures at 8.4 GHz were measured as a function of elevation angle and considering the effects of atmospheric loss, spill-over and stellar body contributions.

A system temperature of 18.7 deg K at 90 deg was measured. The antenna beamwidth at half-power points was found to be 0.067 deg by the drift curve method. In combination with the improved main reflector and subreflector surfaces, the microwave performance of these antennas ranges from 68% to 70% efficiency (67.9 and 68.2 dB gain, respectively). This is a clear increase over the 34-m HA – Dec standard antennas with indicated efficiencies of 49% to 53% (66 to 67.2 dB gain, respectively).

VI. Epilogue

At this time the 34-m Az – El antennas are fully operational at Goldstone and Canberra, and participated in tracking assignments of the highly significant Voyager – Uranus encounter.

They are presently operating in a receive-only mode, at 2 or 8.4 GHz frequencies. At Madrid, the erection and installation of the 34-m Az – El configuration is nearing the mid-point of construction completion. During the remaining installation activity, the configuration will receive a new 8.4-GHz exciter and 20 kW transmitter, and be ready for operational use by April 1987, to support the Galileo and Magellan missions. This added transmit capability is planned for subsequent installation at Canberra and Goldstone in 1987 and 1988.

These highly efficient, highly reliable antennas represent full use of current technology and add significantly to the expected successful deep space encounters during the ensuing decades.

Table 1. Antenna specifications and characteristics

Item	Performance
Antenna Size and Type	34-m, Azimuth – Elevation, Wheel Track
Antenna Weight on Az Axis	345,455 kg (760,000 lb)
Antenna Weight on El Axis	181,818 kg (400,000 lb)
RSS Pointing Error:	
Gravity Plus 30 mph Winds	0.017 deg
Compensated Plus 10 mph	0.004 deg
Compensated Plus 30 mph	0.010 deg
RMS Surface Accuracy:	
Gravity	0.6604 mm (0.026 in.)
Gravity Plus 10 mph Winds	0.635 mm (0.025 in.)
Gravity Plus 30 mph Winds	0.764 mm (0.030 in.)
Locked Rotor Frequency	1.8 Hz
Stability Ratio	1.7 Against Overturning
Balance Structure	Within 6929 m • kg (50,000 ft • lb)
Quadripod Frequency	1.0 Hz
Panel Accuracy	252 0.3049-mm (0.012-in.) RMS Solid Surface Panels to 26-m Diameter. 96 Porous (40% Porosity) Panels to 34-m Diameter.
Panel Strength	136 kg (300 lb) Shoe – Solid Panels 91 kg (200 lb) Shoe – Porous Panels
Aperture Blockage	Maximum of 5%
Subreflector Positioner	2-Axis Automatic Plus 3-Axis Mechanized
Subreflector	Surface Axes Coincide With Mirror Within 10 s Accuracy to Be Within 0.1274 mm (0.005 in.) RMS
Axis Rates	Slew – 0.8 deg/s Track – 0.4 deg/s
Environment	Operational – To 72 kmph (45 mph) Drive to Stow – 80 kmph (50 mph) Hold Any Position – 112 kmph (70 mph) Survive Stowed – 160 kmph (100 mph)
Encoders	Resolution – 0.000343 deg Static Accuracy – 0.00275 deg Repeatability – 0.000343 deg Stability – 0.000343 deg
Loop Closure	0.000343 deg
Overshoot	Zero deg for Step Commands of ±0.00417 deg
Position Loop Bandwidth	0.25 Hz
Antenna Frequency	8.4 GHz
Antenna Gain	67.9 dB to 68.2 dB
Antenna Temperature	18 deg K at Zenith, 23 deg K at Horizon
Cost	About $4,800,000 (1986 US Dollars)
Fire Protection	Automatic Halon Suppression System on Antenna Building and Feed Cone. Dry Standpipe on Antenna. Sprinklers in Cable Wrap Up.
Heating, Ventilation and Air Conditioning	Automatic Controlled System with Economizer, Can Be Remotely Controlled. Energy Efficient Motors Used.

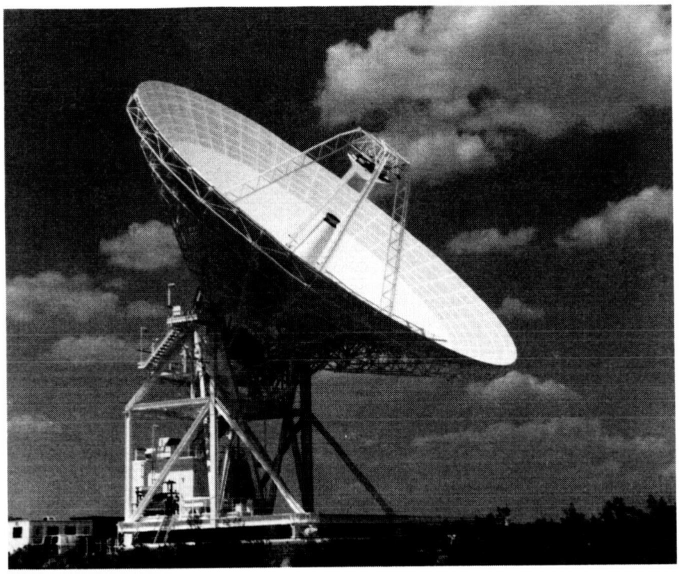

Fig. 1. 34-m Az—El antenna, DSS 15

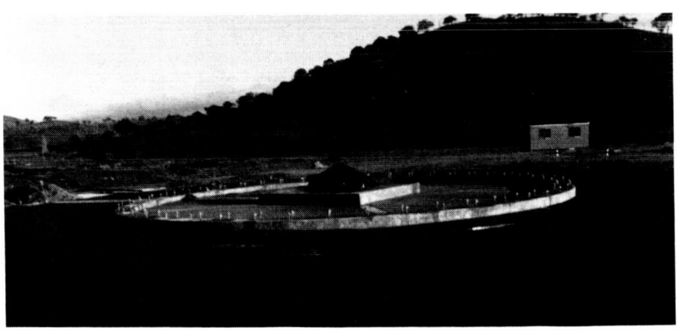

Fig. 2. Foundation, 34-m Az—El antenna, DSS 45

Fig. 3. Track foundation and runner support

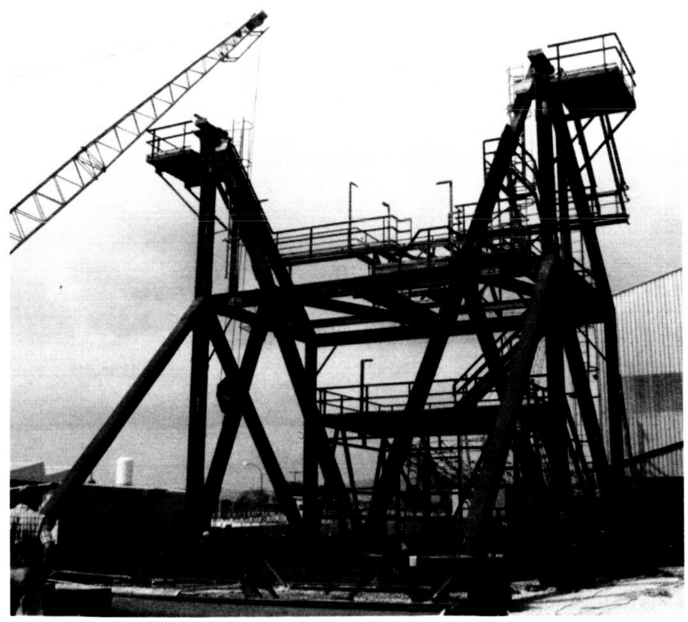

Fig. 4. Alidade structure assembly fit-check, DSS 65

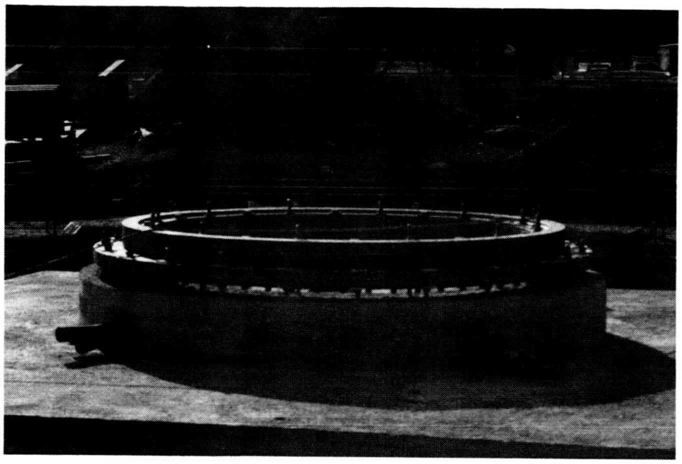

Fig. 5. Pintle bearing and support, DSS 65

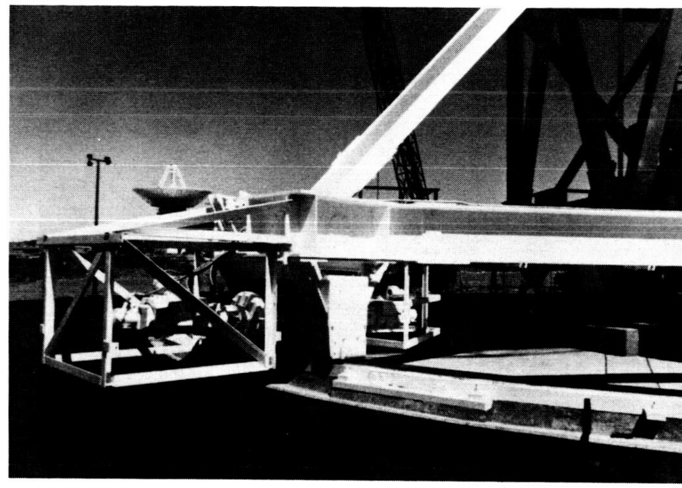

Fig. 7. Azimuth wheel and drive motors, DSS 15

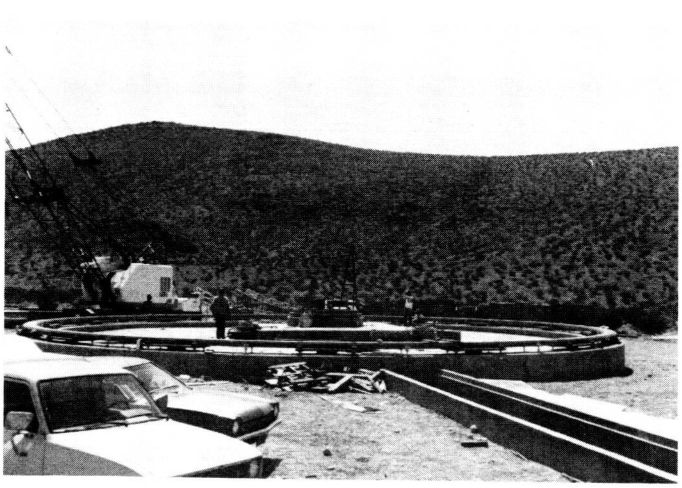

Fig. 6. Track and support runner, DSS 15

Fig. 8. Tipping structure support and elevation bearing

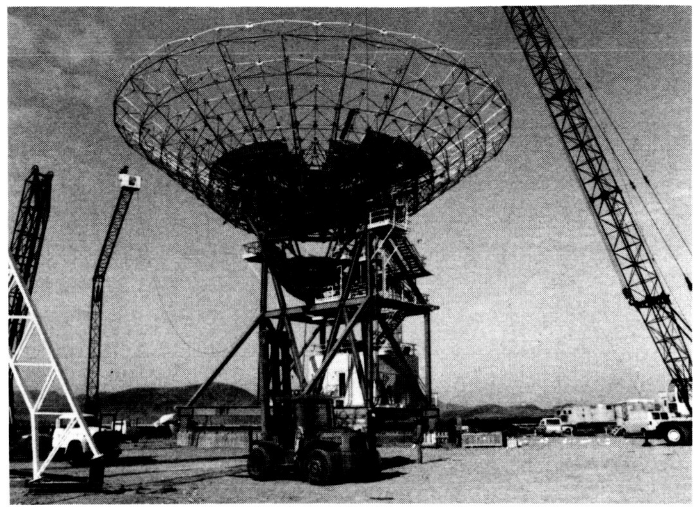

Fig. 10. Reflector and panel support, DSS 15

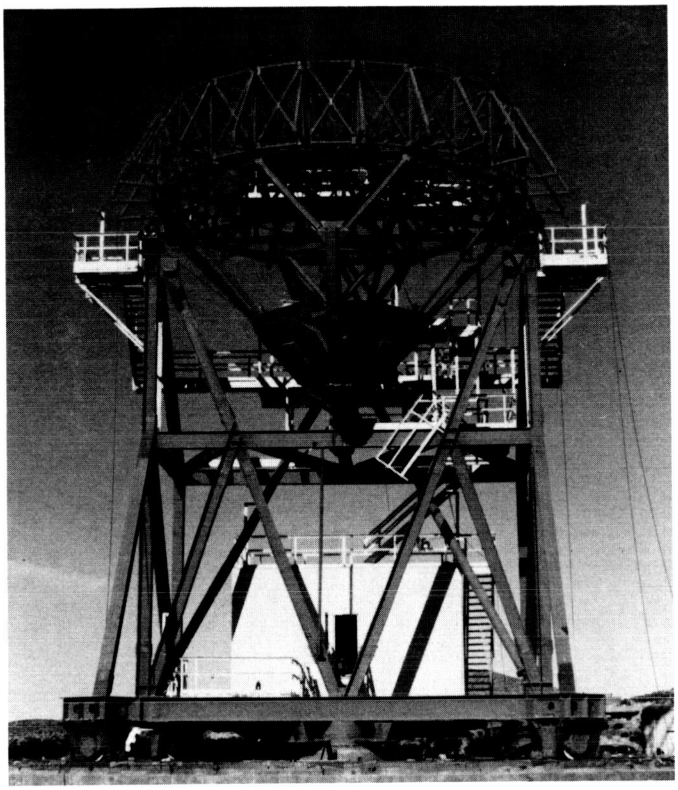

Fig. 9. Main reflector support structure, DSS 15

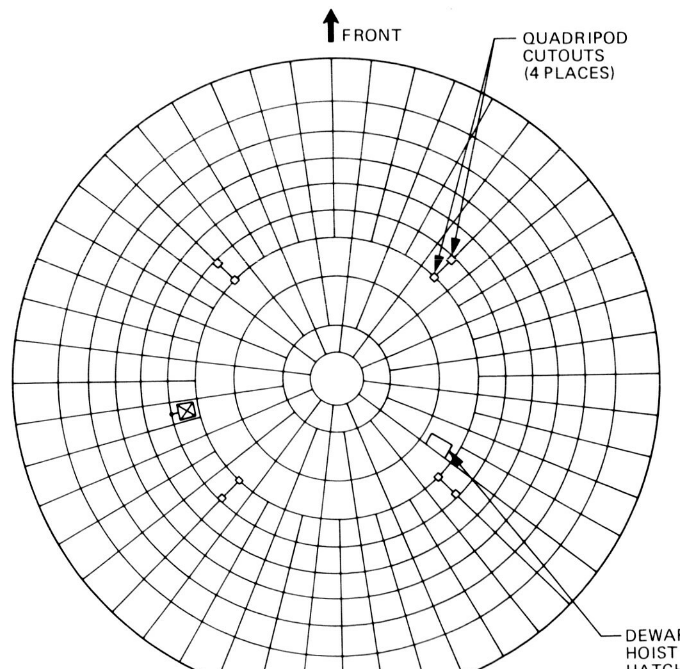

Fig. 11. Reflector panel assembly, from zenith down, DSS 15

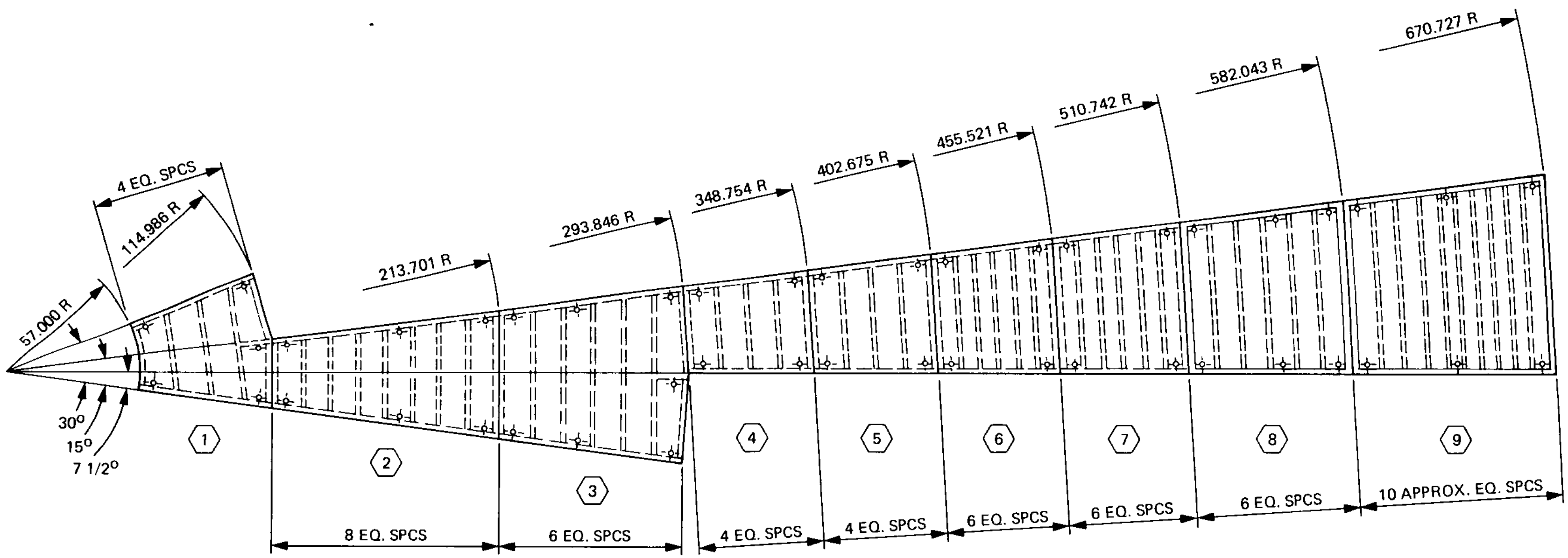

Fig. 12. Typical reflector panel sector, DSS 15

ORIGINAL PAGE IS
OF POOR QUALITY

ORIGINAL PAGE IS
OF POOR QUALITY

Fig. 13. Quadripod structure, DSS 15

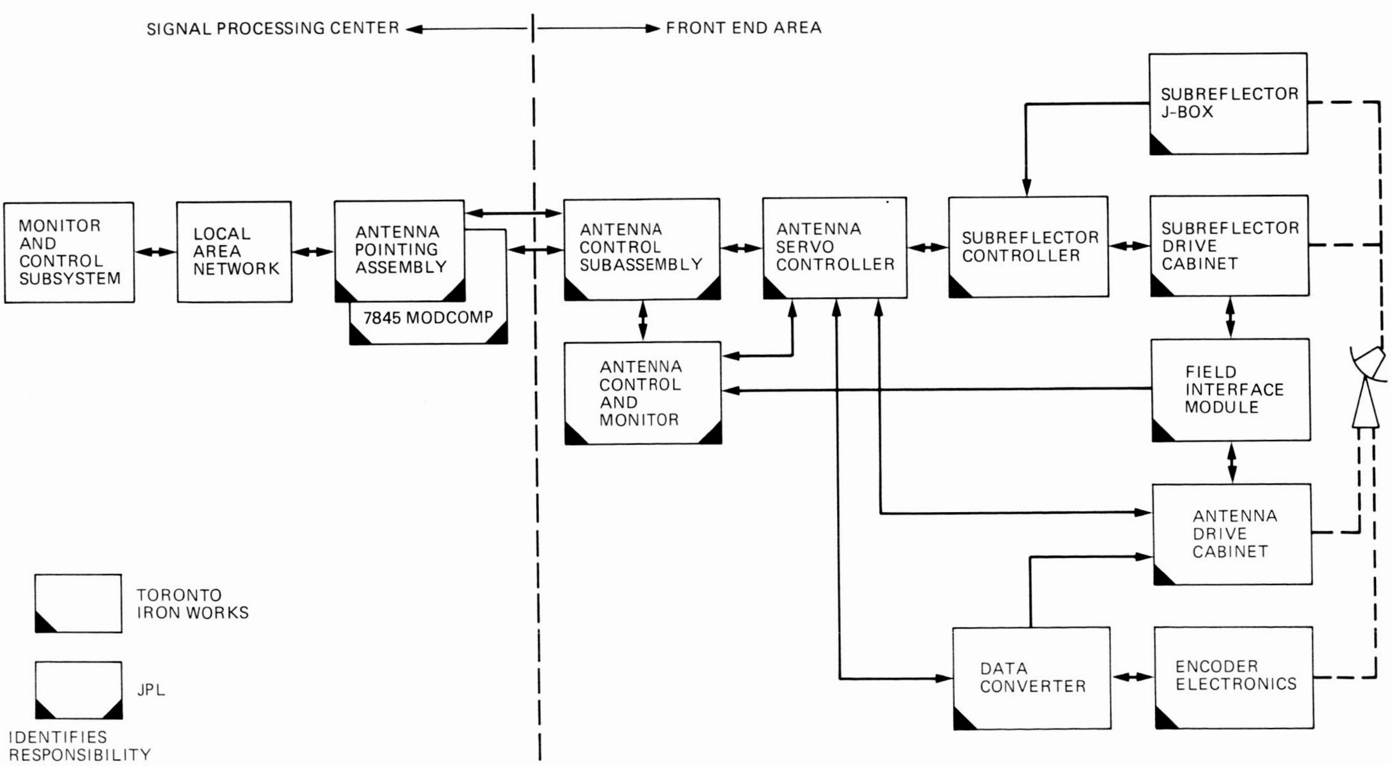

Fig. 14. Block diagram of the antenna control assembly